Addition of a fast GC to SIFT-MS for analyses of individual monoterpenes in mixtures

Michal Lacko[1,2], Nijing Wang[3], Kristýna Sovová[1], Pavel Pásztor[1], Patrik Španěl[1]

[1]The Czech Academy of Science, J. Heyrovský Institute of Physical Chemistry, Dolejškova 2155/3, 182 23 Prague, Czech Republic
[2]Faculty of Mathematics and Physics, Charles University in Prague, Ke Karlovu 3, 121 16 Prague, Czech Republic
[3]Air Chemistry Department, Max-Planck-Institut für Chemie, Hahn-Meitner-Weg 1, 55128 Mainz, Germany

Correspondence to: Michal Lacko (michal.lacko@jh-inst.cas.cz)

Abstract. Soft chemical ionization mass spectrometry (SCI-MS) techniques can be used to accurately quantify volatile organic compounds (VOCs) in air in real time; however, differentiation of isomers still represents a challenge. A suitable pre-separation technique is thus needed, ideally capable of analyses in a few tens of seconds. To this end, a bespoke fast GC with an electrically heated 5 m long metallic capillary column was coupled to a selected ion flow tube mass spectrometry (SIFT-MS) instrument. To assess the performance of this combination a case study of monoterpene isomer ($C_{10}H_{16}$) analyses was carried out. The monoterpenes were quantified by SIFT-MS using H_3O^+ reagent ions (analyte ions $C_{10}H_{17}^+$, *m/z* 137, and $C_6H_9^+$, *m/z* 81) and NO^+ reagent ions (analyte ions $C_{10}H_{16}^+$, *m/z* 136, and $C_7H_9^+$, *m/z* 93). The combinations of the fragment ion relative intensities obtained using H_3O^+ and NO^+ were shown to be characteristic of the individual monoterpenes. Two non-polar GC columns (Restek Inc.) were tested: the advantage of MXT-1 was shorter retention times whilst the advantage of MXT-Volatiles was better temporal separation. Thus, it is possible to quantify components of a monoterpene mixture in less than 45 s by the MXT-1 column and to separate them in less 180 s by the MXT-Volatiles column. As an illustrative example, the headspace of three conifer needle samples was analysed by both reagent ions with both columns showing that mainly α-pinene, β-pinene and 3-carene were present.

1 Introduction

Standard analytical methods used to identify and quantify volatile organic compounds (VOCs) in air, such as thermal desorption gas chromatography mass spectrometry (TD-GC-MS), are often time consuming and cannot be used to investigate temporal changes in chemically evolving systems. In contrast, soft chemical ionization mass spectrometry (SCI-MS) techniques, such as selected ion flow tube mass spectrometry (SIFT-MS) (Smith and Španěl, 2011a; Španěl et al., 2006) and proton transfer reaction mass spectrometry (PTR-MS) (Lindinger et al., 1998; Ellis and Mayhew, 2013; Smith and Španěl, 2011b), represent well-established real time tools to analyse a wide variety of VOCs in ambient air (Amelynck et al., 2013; de Gouw and Warneke, 2007; Rinne et al., 2005; Schoon et al., 2003) and in headspace of biological samples (Shestivska et al., 2015; Shestivska et al., 2011; Shestivska et al., 2012). The advantage of SIFT-MS and PTR-MS lies in the possibility of online,

real-time analysis obviating sample collection and pre-concentration of VOCs. In these techniques, defined reagent ions (usually H_3O^+, NO^+ or $O_2^{+•}$) interact with trace VOCs present in gas samples introduced into a flow tube or a flow/drift tube. The analytical ion-molecule reactions that produced analyte ions are variously proton transfer, adduct ion formation, charge transfer and hydride ion transfer, principally depending on the type of reagent ions used. This ion chemistry has been

5   thoroughly reviewed in a number of publications, e.g. (Smith and Španěl, 2005). These ion-molecule reactions are not greatly exothermic and so few product (analyte) ions are produced in each reaction, often just one or two, that can readily be identified. However, chemically similar molecules with the same atomic composition (structural isomers) usually produce identical analyte ions with similar branching ratios and therefore the neutral analyte molecules cannot be easily differentiated using SCI-MS alone (Smith et al., 2012). However, the reactions of the isomeric molecules may have different rate coefficients with

10   the different reagent ions and lead to product ions at recognisably different branching ratios depending on their molecular geometry (Jordan et al., 2009; Pysanenko et al., 2009; Španěl and Smith, 1998; Wang et al., 2003). So the concurrent use of the available reagent ions in SIFT-MS analysis can sometimes be used to analyse and identify particular isomers.

Monoterpenes, mostly emitted from plants, are very important biogenic volatile organic compounds (BVOCs) in the atmosphere. Due to their high reactivity with atmospheric oxidants such as hydroxyl radicals ($OH^•$), monoterpenes reactions

15   can lead to tropospheric ozone (O_3) accumulation as well as to secondary organic aerosol formation, which can affects human health and contribute to global climate change (Chameides et al. (1992); Fehsenfeld et al. (1992); Kulmala et al. (2004)). Although all monoterpenes comprise two isoprene units and have the same molecular formula, $C_{10}H_{16}$, their reaction time (or lifetime) with $OH^•$ and O_3 widely varies from minutes to days (Atkinson and Arey, 2003). The values of the net BVOC/$OH^•$ reactivity measured in rainforests have been found to be higher than expected, which could be attributed to undetected

20   monoterpenes or sesquiterpenes (Nolscher et al., 2016). Therefore, it is important to identify and individually quantify these BVOCs at their ambient trace levels. Gas chromatography mass spectrometry (GC-MS) coupled with pre-concentration techniques has been developed to successfully identify and quantify different atmospheric monoterpenes (Janson, 1993; Räisänen et al., 2009; Song et al., 2015). However, the requirements of pre-concentration and long cycle time (more than 1h) are obviously unsuitable for real-time measurements.

25   A promising approach to the near real time analysis of isomeric molecules is to combine both SCI-MS and fast GC methods. Pre-separation provided by fast GC involves short columns with thin active layers, fast temperature ramps, fast injection systems and time resolutions below 5 min (Matisová and Dömötörová, 2003). Materic et al. (Materić et al., 2015) established a system using PTR-MS coupled with a fast GC to detect individual monoterpenes in air and achieved the separation of six most common monoterpenes at a limit of detection down to 1.2 ppbv. Pallozzi et al. then compared a fastCG-PTR-ToF-MS

30   system with traditional GC-MS methods, discussing the limitations of the fast GC setup on some BVOCs emitted from plants, including monoterpenes (Pallozzi et al., 2016). SIFT-MS is also widely used in VOCs analyses (Allardyce et al., 2006; Smith and Španěl, 2005b, 2011b). It has well-defined analytical reaction conditions and the H_3O^+, NO^+ and $O_2^{+•}$ reagent ions can be switched rapidly to analyse time-varying trace gases in air samples. In the present article, we report the results of method

development aimed at selective analyses of individual monoterpenes in mixtures in air using a bespoke fast GC/SIFT-MS combination with H_3O^+ and NO^+ reagent ions. This involved the analysis of both prepared laboratory monoterpene/air mixtures and headspace of the foliage of different pine trees.
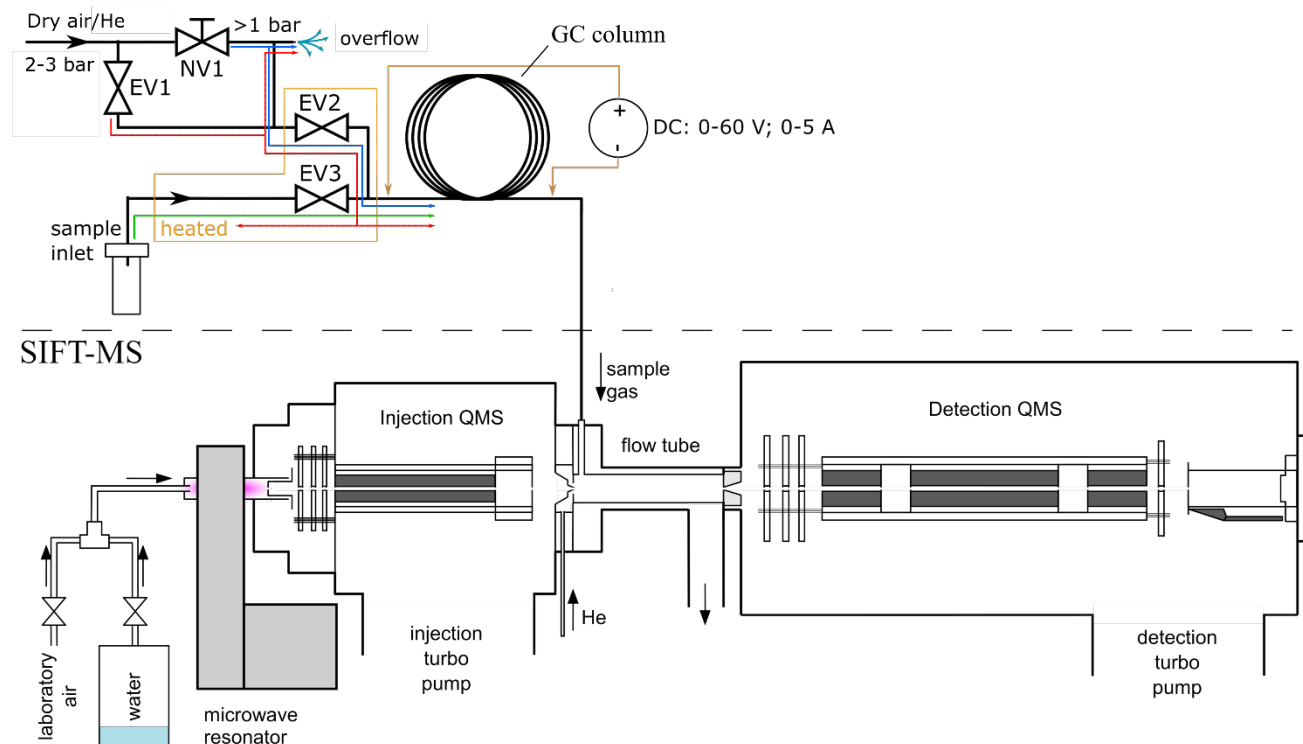
5 **Figure 1: Schematic visualization of the fast GC-SIFT-MS experiment. Coloured dashed lines in the inlet part of the fastCG represent gas flow through the system of the valves EV1-3. The blue line traces the "normal mode" regime, the green line represents the "sampling mode" and the red line represents the "cleaning mode".**

2 Construction of a fast GC device for pre-separation

The experimental setup of the bespoke fast GC setup constructed as an addition to SIFT-MS is shown in **Fig. 1.** In the
10   experiments, two different GC columns were tested. First, a 5 m long nonpolar general-purpose chromatography metallic column MXT-1 (0.28 mm × 0.1 μm active phase, Restek Inc.) using dry air as the carrier gas, which was chosen according to the previous PTR-MS fastGC analyses (Romano et al., 2014). Additionally, a second, application-specific column for volatile organic pollutants, MXT-Volatiles (0.28 mm × 1.25 μm active phase, Restek Inc.) used with helium carrier gas. In order to facilitate direct resistive heating, the coil-shaped stainless steel columns (resistivity ~4.2 Ω/m) were electrically isolated and
15   connected to a regulated 60 V, 5 A DC power supply. Appearance of cold spots was suppressed by ensuring that the electrical current runs through the entire length of the columns. The temperatures of the columns were monitored by a K-type probe

connected to their centres (see the right part of Figure 2 for the temperature variation with applied voltage). It is interesting to note that the flow of sampled air, established by the pressure difference between ambient atmosphere and the low pressure of the SIFT-MS flow tube, changes with the column temperature due to the variation of the dynamic viscosity of the air (see Fig. 2).
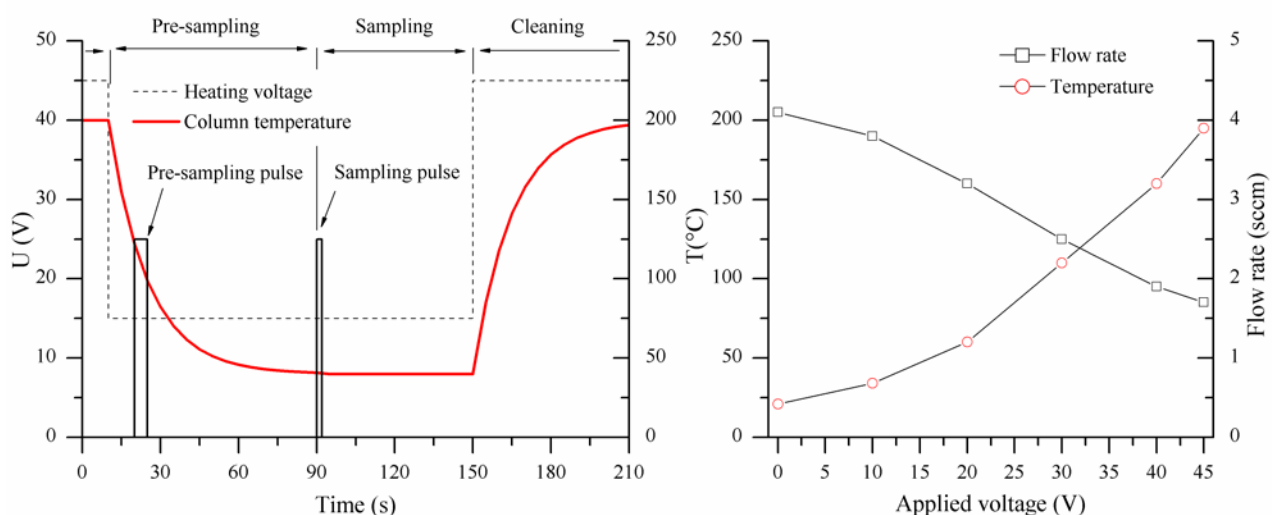
Figure 2: Left: the applied heating voltage (dashed) and the temperature profile of the column (red) during the fast GC cycle. The pulses indicate the opening of the valve EV3 during the pre-sampling and the sampling periods. Right: The increase of the column temperature and the related decrease of the carrier gas flow rate with the heating voltage.

The routing of the sample and the carrier gases was controlled by solenoid valves (Parker VSONC-2S25-VD-F, < 30ms

10 response), labelled in **Fig. 1** as EV1, EV2 and EV3. The needle valve NV1 was used in combination with an overflow relieve tube to fine-adjust the flow rate of the carrier gas (20-50 sccm from a gas cylinder regulator set to about 2 bar) so that the air pressure at the column entrance is held just above ambient. The region of the sampling input line, EV2, EV3 and their connection with the column are permanently heated to ~60 °C to prevent adsorption of sample gas/vapour and to reduce memory effects.

15 Three modes of gas flow are possible as illustrated in Fig. 1:

- The **"normal mode"**: EV2 is open and both EV1 and EV3 are closed. Carrier gas flows through NV1, partly vented via the overflow relieve but mostly into the column. The pressure at the column entrance is just above that of the ambient atmosphere and a constant flow rate of clean carrier gas (synthetic air or helium) is thus achieved.

- The **"sampling mode"**: EV1 and EV2 are closed and EV3 is open. Sample air is introduced into the column in a short
20   time (1 to 8 s) after which the "normal mode" is resumed.

- The **"cleaning mode":** All valves are open and the carrier gas taken directly from the cylinder regulator is introduced into the column (higher than normal flow) and purges the sample line via EV3. The overflow relieve flow rate is not sufficient to diminish the pressure.

The modes can be switched either manually or controlled from the SIFT-MS software.

2.1 The fast GC operation

The operation sequence for air analysis is as follows: A column is first heated up to 200 °C in the "cleaning mode" for three minutes prior to commencing the "normal mode" with an appropriate heating voltage setting (e.g. 10 V as shown in **Fig. 2**). Whilst the column cools down, a pre-sampling interval (8-10 s "sampling mode", see Figure 2) is activated in order to refill the "dead volume" comprising the EV3 valve and the sampling inlet by air at its entrance. After the column reaches working temperature and a steady flow of clean carrier gas is established, the sample for actual analysis is introduced by enabling the "sampling mode" for 1 to 8 s. The GC separation then takes place over typically 60 – 300 s whilst the eluent is continuously analysed by SIFT-MS. It is possible to apply a heating ramp during this period.

In the initial tests with the first generic **MXT-1 column**, the "sampling mode" duration was fixed at 1.8 s due to SIFT-MS software limitations. For the later tests with the second **MXT-Volatiles column**, the SIFT-MS operational software was upgraded to provide an arbitrary timing of the "sampling mode" duration. Sampling was repeated several times to improve sensitivity.

Several heating ramp profiles were tested (see data for MXT-1 column in **Fig. S1** in the Supplement); however, due to the short GC column and relatively long injection time, the monoterpene chromatogram peaks coalesced when the column temperature exceeded 60 °C and it was found that optimal chromatograms were obtained isothermally at 40 °C (15 V heating voltage). Effects of the heating voltage on the retention time and the chromatogram profile are illustrated in **Fig. S3** in the Supplement (data for MXT-Volatiles column).

3 SIFT-MS analyses of the eluent

In the present study, the *Profile 3* SIFT-MS instrument (Instrument Science, Crewe, UK) was used (Smith et al., 1999). Reagent ions are formed in a microwave discharge through a mixture of water vapour and atmospheric air at a pressure of about 0.3 mbar (see Fig. 1). A mixture of ions is extracted from the discharge and focused into a quadrupole mass filter where they can be analysed according to their mass-to-charge ratio, *m/z*. Thus, the reagent ions H_3O^+, NO^+ or $O_2^{+\bullet}$ can be selected ($O_2^{+\bullet}$ was not used in the present experiment) and separately injected into flowing helium carrier gas (pressure $p = 1.4$ mbar, temperature $T = 24$ °C). Any internal energy possessed by the reagent ions is rapidly quenched in collisions with helium atoms leaving a thermalized ion swarm that is convected down the flow tube. Sample gas is introduced into the helium/thermalized swarm at a known flow rate that changes with the GC column temperature. The reagent ions react with the VOC molecules in the sample gas during a time period defined by the known flow speed of the ion swarm and the length of the flow tube. At the end of the

flow tube, the reagent ions and the ionic products (analyte ions) generated by ion-molecule reactions are sampled by a pinhole orifice into the analytical quadrupole mass spectrometer. The count rates of the reagent and analyte ions are obtained using a channeltron multiplier. Thus, full scan (FS) spectra can be obtained over a chosen m/z range to identify the analyte ions or rapidly switched between selected m/z values using the multiple-ion monitoring mode (MIM) (Španěl and Smith, 2013; Smith

5   and Španěl, 2011a). For the monoterpene study, the FS mode was used for SIFT-MS analyses, whilst the MIM mode was used for fast GC-SIFT-MS setup.

3.1 Reactions of H_3O^+ and NO^+ reagent ions with monoterpenes

In the present study, SIFT-MS analyses of monoterpenes were carried out using the previously investigated reactions of monoterpenes with H_3O^+ and $NO^{+\cdot}$ ions (Schoon et al., 2003; Wang et al., 2003). The H_3O^+ reactions are known to proceed via

10   proton transfer forming $C_{10}H_{17}^+$ (m/z 137) that partially fragments to $C_6H_9^+$ (m/z 81) due to elimination of a C_4H_8 moiety from the nascent $(C_{10}H_{17})^*$ excited ion:

$$H_3O^+ + C_{10}H_{16} \rightarrow C_{10}H_{17}^+ + H_2O \tag{1a}$$
$$\rightarrow C_6H_9^+ + C_4H_8 + H_2O \tag{1b}$$

NO^+ reacts with monoterpenes by charge transfer forming the parent cation $C_{10}H_{16}^{+\cdot}$ (m/z 136) and a number of fragment ions,

15   including $C_7H_9^+$:

$$NO^+ + C_{10}H_{16} \rightarrow C_{10}H_{16}^+ + NO \tag{2a}$$
$$\rightarrow C_7H_9^+ + NOC_3H_7 \tag{2b}$$

The exothermicity of charge transfer (2a) is represented by the difference between the ionization energies of the neutral NO (9.26 eV) and of the particular monoterpene (ranging from 8.07 eV for α-pinene to 8.4 eV for (R)-(+)-limonene) (Garcia et al.,

20   2003; NIST). Other fragments, including $C_7H_8^+$, $C_7H_{10}^+$, $C_9H_{13}^+$ and $C_{10}H_{15}^+$, are also formed and the branching ratios between the channels (2a) to (2b) and other fragments depend on the isomeric structure of the monoterpene (Schoon et al., 2003; Wang et al., 2003) and are given in **Table S1** in the Supplement. Based on this known ion chemistry, for the present study it was decided to analyse monoterpenes using both the H_3O^+ reagent ions by recording the $C_{10}H_{17}^+$ (m/z 137) and $C_6H_9^+$ (m/z 81) analyte ions and the NO^+ reagent ion by using the $C_{10}H_{16}^+$ (m/z 136) and $C_7H_9^+$ (m/z 93) analyte ions. To facilitate the

25   identification of monoterpenes on the basis of the branching ratios of reactions (1) and (2), the product ion signal ratios [m/z 81]/[m/z 137] and [m/z 93]/[m/z 136] were determined under the conditions of the *Profile 3* SIFT-MS instrument using standard monoterpene mixtures, and these ratios (r) are given in **Table 1**.

The interaction of the primary ions with monoterpenes may be affected by the presence of neutral water molecules, and thus by different humidity of the sample, as reported previously by Wang et al. (Wang et al., 2003) when decreased fragmentation

30   of monoterpene product ions was observed in humid air samples. For H_3O^+ regent ions, this change was significant for β-pinene (r reducing from 0.75 to 0.51), (R)-(+)-limonene (r from 0.45 to 0.34) or 3-carene (r from 0.33 to 0.23). For the NO^+ regent ion, a significant effect was observed only for α-pinene (r from 0.32 to 0.08) and β-pinene (r from 0.25 to 0.05).

3.2 Analysis of the product ion intensity ratios

To facilitate assignment of the fast GC elution peaks to specific monoterpenes, mean fragment ion fractions $r_i = f_i/g_i =$ [m/z 81]/[m/z 137] (or for NO$^+$, $r_i = f_i/g_i =$ [m/z 93]/[m/z 136]) were calculated for each interval of retention times t_1 to t_2, as the weighted mean of the product ion signal ratios $\overline{r_w}$:

$$5 \quad \overline{r_w} = \sum_{i=t_1}^{t_2} w_i \frac{f_i}{g_i}; \; w_i = \frac{f_i+g_i}{\sum_{i=t_1}^{t_2} f_i+g_i}, \quad (3)$$

The weights (w_i) applied to each of several discreet measurements were based on the total signal of both ions f_i and g_i in order to emphasise the area within the peak. Time intervals t_1 to t_2 were chosen for each isomer as the area of the chromatographic peak where the total ion signal was >10% of the peak value.

The quality of the ratio estimation was assessed from the variation of the f_i/g_i ratio estimated as:

$$10 \quad \sigma_i^2 = Var(f/g) \approx \frac{\mu_f^2}{\mu_g^2}\left(\frac{\sigma_f^2}{\mu_f^2} + \frac{\sigma_g^2}{\mu_g^2}\right) = \frac{\mu_f^2}{\mu_g^2}\left(\frac{\lambda_f+\sigma_{bg_f}^2}{\mu_f^2} + \frac{\lambda_g+\sigma_{bg_g}^2}{\mu_g^2}\right), \quad (4)$$

where μ_f and μ_g represent intensities of the selected fragments and σ_f^2 and σ_g^2 are the variances of the μ_f and μ_g intensities estimated according to the Poisson distribution as the sum of distribution variance equal to the expected value $\lambda = \mu$ and background variance σ_{bg}^2 (Van Kempen and Van Vliet, 2000).

From this variation, the standard error of the weighted mean was calculated as:

$$15 \quad \sigma_{\overline{r_w}} = \sqrt{\sum_{i=t_1}^{t_2} w_i^2 \sigma_i^2} \quad (5)$$

The weighted standard deviation of the f_i/g_i ratios was also routinely calculated as:

$$s = \sqrt{\frac{\sum_{i=t_1}^{t_2} w_i\left(\frac{f_i}{g_i}-\overline{r_w}\right)^2}{1-\sum_{i=t_1}^{t_2} w_i^2}} \quad (6)$$

3.3 Reference chemicals and plant samples

All monoterpenes used in the experiments, viz. ((+)-α-pinene (98%), (+)-β-pinene (≥98.5% analytical standard), camphene
20 (95%), myrcene (≥90% analytical standard), 3-carene (≥98.5% analytical standard), (R)-(+)-limonene (≥99.0% analytical standard), α-terpinene (≥95%) and γ-terpinene (97 %), were purchased from Sigma-Aldrich Co. Individual monoterpene vapour standards and monoterpene vapour mixtures were prepared by the diffusion tube method (Thompson and Perry, 2009). Thus, for individual standards, about 5 µl of each monoterpene was placed in a 2 ml vial closed by PTFE septum caps. Each vial was then penetrated with a diffusion tube (1/16" OD x 0.25 mm ID x 5 cm length PEEK capillary) and placed into a 15 ml
25 glass vial closed by a PTFE septum. The headspace of the 15 ml vial was sampled after stabilization (> 30 minutes) of the concentration. Humidity of the headspace was typically 1.5% water vapour by volume as determined by SIFT-MS. For the α-pinene, the intensities were too high and thus they had to be reduced by placing only trace amount of sample into the 2 ml vial. For the mixture preparations, a similar approach was used; several vials containing different monoterpene liquid samples,

penetrated by PEEK capillaries, were placed together into a 500 ml bottle. Note that the concentrations of the individual isomers in the mixture are different due to the variations in their saturated vapour pressures.

To demonstrate the applicability of the fast GC/SIFT-MS analyses to real samples, three different species of coniferous tree needles were prepared: Spruce (*Pincea punges*), Fir (*Abies concolor*) and Pine (*Pinus nigra*) (see **Fig. S4 – S6** in the Supplement). For the first study using the MXT-1 column, the needle samples (0.26 g Spruce, 0.42 g Fir and 0.32 g Pine) were collected in the urban area of Prague in June 2017 and stored in 10 ml vials from which the headspace was sampled. For the later study using the MXT-Volatiles column, pine tree twigs were collected in June 2018 from the same trees (21.8 g Spruce, 21.4 g Fir and 20.6 g Pine). The exposed cuts of the twigs were sealed by parafilm. The samples were placed into a Nalophan bag of volume approximately one litre. During the analyses, the laboratory was thermalized to the outdoor temperature (about 30 °C) to reduce thermal shock to the samples.

4 Results and discussion

To assess whether the various monoterpenes in a mixture could be effectively distinguished using SIFT-MS enhanced by the fast GC pre-separation, eight common biogenic monoterpenes were investigated, as identified in 3.3 above. The mixture of monoterpene standards was analysed using isothermal GC with two different columns at temperature of 40 °C. The elution times of all eight monoterpenes were within 45 s of total retention time for the **MXT-1 column** and within 180 s for the **MXT-Volatiles column**. Using the information on the ratios of the ion products for the H_3O^+ and NO^+ reactions together with the GC retention times, it was possible to identify the components of the reference mixture. Finally, the same procedure was used to analyse the three fresh pine tree needle samples.

4.1 Comparison of columns: MXT-1 vs. MXT-Volatiles

The retention times determined from the chromatograms obtained for individual monoterpenes are given in **Table 1** together with their $\overline{r_w}$ values (see equation 3). For the MXT-1 column, the apparent difference in retention times observed between the two reagent ions was probably caused by the temperature fluctuations of the column. Whilst the retention times for individual monoterpenes are different, they are not sufficiently stable (fluctuate by > 1 s, see **Table 1**) in the present fast GC device for analyses based on retention time only to be reliable. Use of the MXT-Volatiles column resulted in about five times longer retention times and better GC peaks separation at the same operational conditions (flow rate, temperature and pressure) due to the higher efficiency of the 1.25 μm active phase (compared to 0.1 μm for MXT-1 column). Due to the different sampling times used with each column (1.8 s for MXT-1 and 5 to 12 s for MXT-Volatiles), the peak shapes cannot be compared directly but the peak width (FWHM) increased only two times for the MXT-Volatiles column.

The performance of both MXT-1 and MXT-Volatiles columns were compared by analyses of a gas mixture of the eight monoterpenes. For the MXT-1 column, four characteristic GC peaks were identified for both reagent ions, marked as A, B, C and D with retention time of 17.6 s, 20.8 s, 26.3 s and ~30 s for H_3O^+, and 17.5 s, 20.7 s, 26.3 s and ~30 s for NO^+ (see **Fig. 3**).

Based on the retention times obtained for individual monoterpenes (see **Fig. S2** in the Supplement), peak A is due to co-elution of α-pinene, camphene and myrcene. Peak B is due to the presence of β-pinene exclusively and peaks C and D are due to the remaining four monoterpenes. Note that the individual peak heights are influenced by the monoterpene saturated vapour pressures (see **Table 1**). Using the MXT-1 column under these conditions it was not possible to achieve separate GC peaks for

5 individual monoterpenes, however qualitative analysis was possible.

Table 1: Ratios of the H_3O^+ and NO^+ reaction product ion signals and the GC retention times, s, for the eight monoterpenes at columns temperature 40 °C. Also given are the saturated vapour pressures in Torr. The standard error of the fast GC $\overline{r_w}$ values for individual monoterpenes estimated by Eq. (5) is less than 5% (except 8.6% for camphene), overall less then ±0.02.

| Compound | [m/z 81]/[m/z 137] | | [m/z 93]/[m/z 136] | | Retention time [s] | | |
| | H₃O⁺ | | NO⁺ | | H₃O⁺ | NO⁺ | H₃O⁺ |
Saturated vapour pressure (Torr)	Literature _Schoon_[a] _Wang_[b]	Results _Full scan fast GC MIM_	Literature _Schoon_[a] _Wang_[b]	Results _Full scan fast GC MIM_	MXT-1	MXT-1	MXT-Vol
α-pinene 4.75[e]	0.45	0.67[c]	0.05	0.16[c]	16	14.7	72
	0.64	0.46[d]	0.09	0.19[d]			
camphene 2.50[e]	0.1	0.14[c]	0	-	17	17.7	83
	0.16	0.16[d]	0.01	0.03[d]			
β-pinene 2.93[e]	0.52	0.61[c]	0.03	0.12[c]	20.4	22	106
	0.67	0.66[d]	0.08	0.17[d]			
myrcene 2.09[f]	0.44	0.72[c]	0.36	0.72[c]	18.5	17.8	134
	0.52	0.51[d]	0.62	0.63[d]			
3-carene 3.72[h]	0.24	0.39[c]	0.05	0.12[c]	25.5	25.6	142
	0.32	0.35[d]	0.1	0.15[d]			
α-terpinene 1.64[h], 1.66[i]	-	0.14[c]	-	0.01[c]	27	25.1	157
	0.11	0.17[d]		0.01[d]			
(R)-(+)-limonene 1.98[g]	0.30	0.43[c]	0	0.03[c]	27.5	31	170
	0.43	0.41[d]	0.01	0.06[d]			
γ-terpinene 1.07[h], 0.7[j]	-	0.18[c]	0.08	0.08[c]	40.4	32.5	184
	0.21	0.16[d]	0.09	0.09[d]			

[a] (Schoon et al., 2003); [b] (Wang et al., 2003); [c] Present result based on SIFT-MS measurement; [d] Present result based on

10 fast GC-SIFT-MS measurement; saturated vapour pressures in Torr at 25 °C according to [e] (Daubert, 1989), [f] (Haynes, 2014), [g] (Yaws, 1994), [h] (TGSC), [i] (Takasago, 2011), and at 20 °C according to [j] (ChemicalBook, 2016).
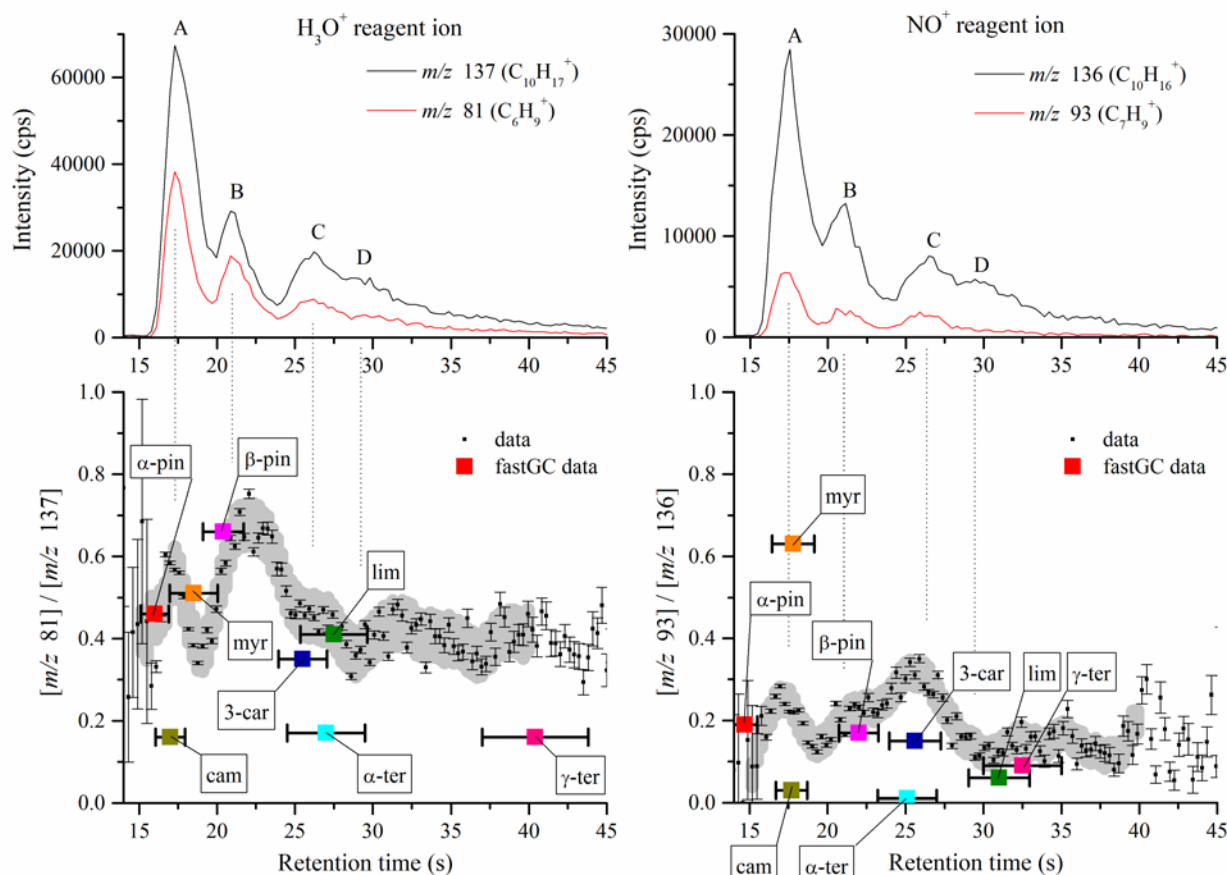
Figure 3: Chromatograms of the mixture of monoterpenes (upper figures) measured by H₃O⁺ (left) and NO⁺ (right) reagent ions, obtained using the MXT-1 column. A, B, C, D represent characteristic peaks in the chromatogram. For each chromatogram, the product ion signal ratio r_i is presented in the lower figures. The grey data background represents the calculated standard deviation of the data by Savizky-Golay smoothing between 15 s and 40 s. The position and value of the ratio for individual monoterpenes is based on the fast GC MXT-1 measurements presented in Table 1. Note that the retention times are determined by the fast GC conditions and do not depend on which SIFT-MS reagent ion is used.

The separation of the chromatographic peaks could be improved using hydrogen or helium as a carrier gas and by faster sample injection, as demonstrated by Materic et al. (Materić et al., 2015) with fastGC PTR-MS, where complete separation of monoterpenes was achieved. As observed for both columns, separation can be improved by decreasing the column temperature (see **Fig. S3** in the Supplement), however this may increase the chromatogram width and thus decrease the sensitivity of the technique. Additional sensitivity can be achieved by increasing the injection time, which will, however, increase the peak width. In the present experiment we used heated columns isothermally to the temperature about 40 °C due to the behaviour of the MXT-1 column. For higher temperatures, the monoterpene chromatogram peaks coalesced. For lower temperatures a significant influence of lab air temperature fluctuations was apparent. Under these conditions for the MXT-1 column,

monoterpenes are not fully separated and thus, the fast GC with the MXT-1 column alone (at 40 °C) provides only qualitative analysis.

The MXT-Volatiles column facilitates identification of all monoterpenes present in the mixture for temperatures close to room temperature (**see Fig. S3** in the Supplement). For the MXT-Volatiles tests, the sampling mode was extended to 12 s,

5 representing the collection of approximately 0.6 ml of the monoterpene mixture headspace. A noticeable effect of ambient temperature on the rate of passive column cooling was observed resulting in changes of the column temperature profile and thus in variations of the monoterpene retention times. It is interesting to note that the chromatogram (**see Fig. S3** in the Supplement) changes with the temperature of the column and additional peaks appear at higher temperatures probably resulting from the presence of different conformers. It thus seems that at the column temperature ~45 °C using 20 V heating voltage

10 (see **Fig. 4**) the small β-pinene is hidden behind the second camphene peak and the α-terpinene peak also disappears (see also the fragmentation analyses later in section 4.2).
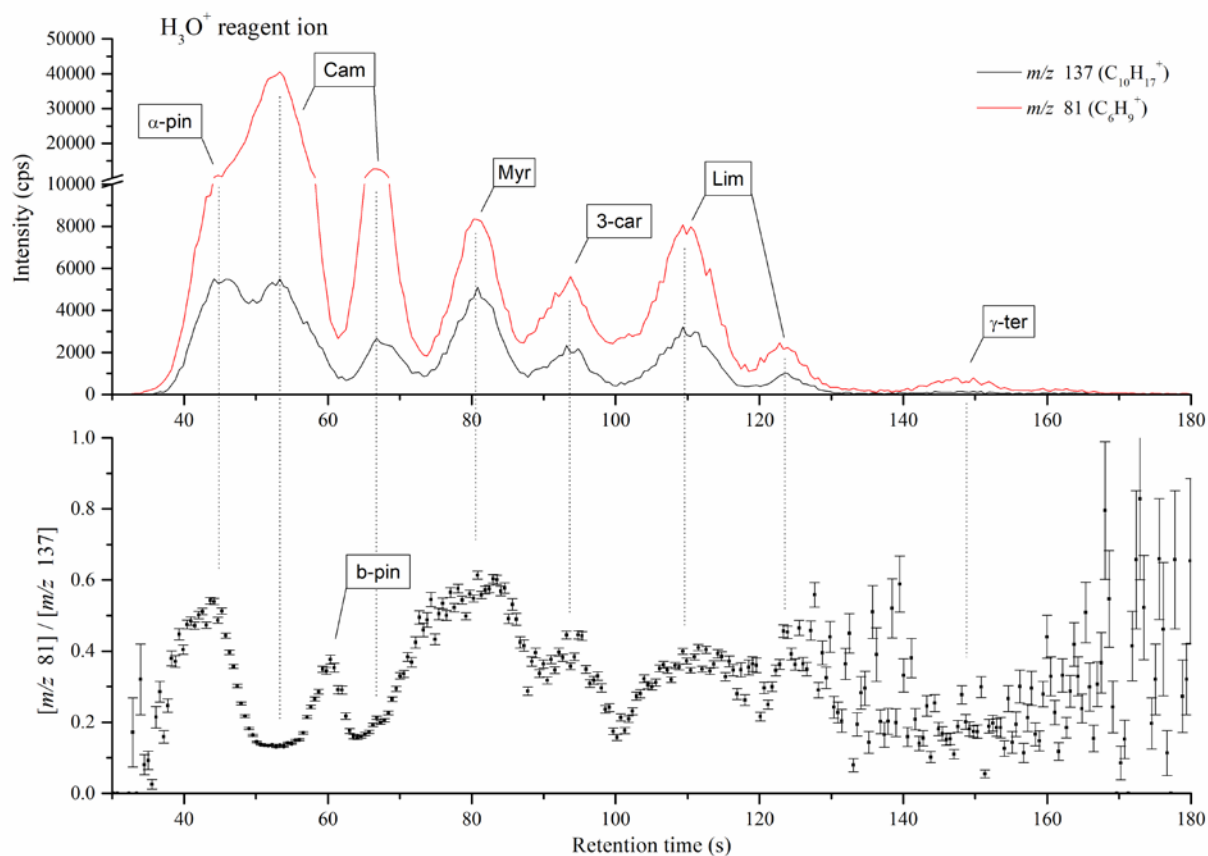
Figure 4: A chromatogram for a prepared mixture of monoterpenes obtained with the MXT-Volatiles column as derived by SIFT-MS using H_3O^+ reagent ions. For the chromatogram, the product ion signal ratio r_i is presented in the bottom figure. This
15 **chromatogram was obtained at the column temperature ~45 °C using 20 V heating voltage.**

4.2 Use of NO$^+$ reagent ions for improved selectivity

Inadequacies in separation of monoterpenes due to a short column or high temperature can be mitigated by using an additional reagent ion and by the analysis of the product ion signal ratios r_i (see **Sec. 3.2**). It may be possible to improve identification of myrcene as well as of other monoterpenes by exploiting different ion chemistry of the NO$^+$ regent ions compared to H$_3$O$^+$ reagent ions. The NO$^+$ data in combination with H$_3$O$^+$ data allow identification of compounds on the basis of four different product ion ratios. Note that the retention times are determined by the fast GC conditions and do not depend on which SIFT-MS reagent ion is used (see **Table 1**).

It must be kept in mind, that monoterpenes are not the only BVOCs emitted by plants. When plants are physically damaged, they emit so called „leaf aldehydes" such as 2-, and 3-hexenal (Tani et al., 2003). The ion chemistry of these two aldehydes differs in SIFT-MS. Whilst the reaction of 2-hexenal with H$_3$O$^+$ proceeds via proton transfer forming a product ion at *m/z* 99 (100 %), it has been found that reaction of cis-3-hexenal with H$_3$O$^+$ results in H$_2$O elimination producing a dominant fragment ion at *m/z* 81 (Španěl et al., 1997) as do the H$_3$O$^+$/monoterpene reactions. To avoid an overlap of 3-hexenal with monoterpenes, it is thus more reliable to use the product ion at *m/z* 137 for the H$_3$O$^+$/monoterpene reactions. Another approach is to choose NO$^+$ as a precursor ion, where the product ions of 3-hexenal (*m/z* 97, 69 and 74) do not overlap with those of monoterpenes (*m/z* 92, 93 and 136) (Wang et al., 2003). A similar approach can be applied to other isomeric or isobaric molecules present in the environment like isoprene that form a product ion at *m/z* 69, overlapping with the second hydrate of methanol that is also emitted by plants (12% of global BVOC emissions) (Španěl et al., 1999).

The $\overline{r_w}$ values obtained from the SIFT-MS FS data and the MIM data for the fast GC peaks for most of the isomers are in good agreement. However, the ratios obtained for α-pinene and myrcene are somewhat variable between the FS and MIM data and they also differ somewhat from the literature values. This may be caused by a different humidity of the samples, as discussed in Section 3.1., where it was seen that increase of humidity lowered the $\overline{r_w}$ values. The greatest fluctuation was observed for myrcene, which was not found to be sensitive to humidity, in contrast to the sensitive compounds (β-pinene, (R)-(+)-limonene and 3-carene for H$_3$O$^+$ regent ion, and α-pinene, β-pinene NO$^+$ regent ion). The standard error of the fast GC $\overline{r_w}$ values for individual monoterpenes estimated by Eq. (5) (using the MXT-1 column) is less than 5% (except 8.6% for camphene) and is smaller than the observed variability between the methods. The $\overline{r_w}$ values for MXT-Volatiles column were similar to those obtained with MXT-1 column, as expected.

The $\overline{r_w}$ values for peaks A, B, C and D were calculated as 0.49, 0.63, 0.45, 0.40 respectively for H$_3$O$^+$ and as 0.21, 0.21, 0.27, 0.14 for NO$^+$. Based on these ratios (using **Table 1**), peak B can clearly be assigned as β-pinene. However, the remaining peaks contain several isomers and thus, the $\overline{r_w}$ values do not provide unique identifications. So dynamic variations of r_i need to be investigated to see if they can provide additional information.

The time profile of r_w is shown in the bottom part of Fig. 3. To recognize trends in these data, Savizky-Golay smoothing (Savitzky and Golay, 1964) was used (second polynomial order across 10 data points, OriginPro 9.0 (OriginPro, 2018). Also plotted (grey area in **Fig. 3**) is the standard deviation of the data points from the smoothed line in the interval of retention times

from 15 s to 40 s. Note that this standard deviation is greater than the standard error of the data points, possibly due to a lower accuracy of data at the longer retention times. The standard deviation allows assessment of the significance of the changes in $r_i = f_i/g_i$.

According to the elution time, the first chromatographic peak A consist of three monoterpenes: α-pinene, camphene and

5   myrcene. For the H_3O^+ reagent ions, the $\overline{r_w}$ value corresponds to both α-pinene and myrcene considering the $\overline{r_w}$ value for peak A (0.49) or r_w close to the peak maxima (0.55–0.6). However, a more obvious difference between α-pinene and myrcene is observed with the NO^+ reagent ions. The value of the weighted mean ratio for the peak A (0.21) is close to the ratio for α-pinene. In the maxima of peak A, however, r_w approaches the value of 0.3, which is close to the value expected for a combination of both these monoterpenes (0.32, considering the data from fast GC measurement and the vapour pressure in

10 Table 1). For camphene, r_w in the chromatograph did not reach the low values expected for both reagent ions. However, its presence is clearly visible as a dip in r_w situated between the peaks A and B. In the absence of camphene, the ratio should linearly move to values characteristic for the peak B without any dip. The depth of the dip does not reach the ratio expected for camphene due to a persistent tails of the peaks for both α-pinene and myrcene.

Peak B in the chromatograms is identified as β-pinene by its retention time. The $\overline{r_w}$ values for the H_3O^+ and NO^+ reagent ions

15 are 0.63 and 0.21, respectively. The values r_w are similar to $\overline{r_w}$ and slightly higher than to the fast GC standard values for β-pinene (see **Table 1**).

Peaks C and D are not clearly separated in the chromatogram. For the H_3O^+ reagent ions, the $\overline{r_w}$ value is similar for both peaks; thus, the presence of (R)-(+)-limonene, 3-carene or α-terpenine is likely since the $\overline{r_w}$ values for the peaks C (0.45) and D (0.4) are comparable with the analyte signal ratios (see **Table 1**) for (R)-(+)-limonene and 3-carene. A lower r_i for α-terpinene might

20 be observed as a dip similar to that for camphene. However, the observed dip in r_i at the D peak is not as statistically significant as the dip for camphene, and the vapour pressure for both α- and γ-terpine are lower than other monoterpenes. Analysis of the C and D peaks using the NO^+ reagent ion shows a clearer difference between them. The calculated $\overline{r_w}$ for the peak C (0.27) as well as the maximum r_i (0.35) are, unexpectedly, much higher than for the remaining monoterpenes. This can be explained only by the influence of myrcene or by the presence of impurities in the form of an additional monoterpene in the mixture (for

25 example ocimeme has high r_i of 0.62 (Wang et al., 2003)). Amongst the eight monoterpenes, 3-carene has the highest r_i within the retention time of peak C. The second peak D (0.14) can be then associated with (R)-(+)-limonene, which has a low r_i (0.06) for NO^+ reagent ions, with some contribution by α-terpinene. The presence of γ-terpenine is not visible due to its low vapour pressure, but there may be some contribution in the D peak, but much smaller than the contribution by (R)-(+)-limonene.

30 To summarize, combining analyses using both H_3O^+ and NO^+ reagent ions with dynamic variations of r_i allows the identification of α-pinene, camphene and myrcene in peak A followed exclusively by β-pinene in peak B. Peak C is characterized as 3-carene and peak D as (R)-(+)-limonene and/or α-terpinene. γ-terpenine contributes only weakly due to its low vapour pressure and has no recognisable response in the chromatogram compared to the remaining monoterpenes.

4.3 Tree samples investigation using the MXT-1 column

To test the suitability of the fast GC-SIFT-MS combination for analyses of real biological samples, VOC emissions were analysed from three fresh coniferous tree needle samples (spruce, fir, and pine) as shown in **Fig. 5**. Based on the results of the above GC data for standard monoterpene mixtures, the chromatograms were divided into three areas. The first part

5 characterized by the presence of α-pinene, camphene and myrcene between retention times of 12-18 s, the second part characterized by the presence of β-pinene with retention times between 18-25 s and the third part characterized by presence of 3-carene and (R)-(+)-limonene /α-terpenine with retention times between 25-40 s. The $\bar{r_w}$ values were calculated for the selected regions as follows

- Spruce: The first region of the main peak at $\bar{r_w}$ values of 0.35 (H_3O^+), 0.11 (NO^+). Note that the very low $\bar{r_w}$ for NO^+

10 indicates the absence of Myrcene. The $\bar{r_w}$ value for H_3O^+ is lower than expected for β-pinene and higher than expected for camphene. Therefore, the first peak is formed mainly from α-pinene, perhaps with small amount of camphene. The second region of a small peak with 0.38 (H_3O^+) and 0.14 (NO^+). $\bar{r_w}$ for H_3O^+ is lower than expected for β-pinene and higher than that for camphene; the low $\bar{r_w}$ for NO^+ indicates the absence of myrcene; 3-carene is thus the best match. The signal increase in the third region may indicates trace presence of (R)-(+)-limonene.

15 - Fir: The chromatogram shows two intense peaks. The calculations of $\bar{r_w}$ for the first region (0.40 for H_3O^+, 0.14 for NO^+) and for the second region (0.56 for H_3O^+, 0.15 for NO^+) indicate the presence of both α-pinene and β-pinene. The decreasing $\bar{r_w}$ for the H_3O^+ reagent ions in the last part of the chromatogram (0.48 for H_3O^+, 0.19 for NO^+) indicates the presence of an additional monoterpene, 3-carene.

- Pine: Chromatogram contains only one peak. $\bar{r_w}$ is stable for both reagent ions for all retention times: 0.55 for H_3O^+,

20 0.21 for NO^+ for the first sector; 0.57 for H_3O^+, 0.22 for NO^+ for the second sector; 0.57 for H_3O^+, 0.22 for NO^+ for the third sector. Together with the retention time of the peak (16.4 s) this certainly corresponds to α-pinene.

4.4 Tree samples analyses using the MXT-Volatiles column

Similar experiments were conducted also using the MXT-Volatiles column. The retention times for the individual monoterpenes were taken from the standard data obtained at the same column temperature (40 °C). The headspaces of the

25 prepared tree needle samples were sampled for 6 s, each representing a volume of 0.3 ml. The chromatograms obtained for the spruce, fir and pine samples are shown in **Fig. 6** and represent the means of analyte ion count rates from 5 consecutive runs normalized to a constant reagent ion count rate of 10^6 s^{-1}.

For spruce, four peaks were observed in the chromatogram. The first peak with a retention time of 68 s corresponds to α-pinene with $\bar{r_w}$ of 0.60 for H_3O^+ and 0.24 for NO^+ regent ions. The tailing edge of the first peak shows a decrease of $\bar{r_w}$ (0.29 for

30 H_3O^+, 0.14 for NO^+) due to a small contribution by camphene. The second peak corresponds to β-pinene, characterized by a retention time of 94 s with $\bar{r_w}$ of 1.05 for H_3O^+ and 0.50 for NO^+. The standard deviation in r_w was unfortunately substantial (±0.6 for H_3O^+, ±0.73 for NO^+). The position of the third peak corresponds to myrcene. The $\bar{r_w}$ values (0.43 for H_3O^+, 0.41 for

NO$^+$) were again imprecise due to the low intensity and do not fully agree with the unique $\overline{r_w}$ for myrcene (see Table 1). The observed weak peak could therefore be due to other monoterpenes other than those eight included in Table 1. The last peak corresponds to 3-carene with $\overline{r_w}$ as 0.48 for H$_3$O$^+$ and 0.16 for NO$^+$ reagent ions
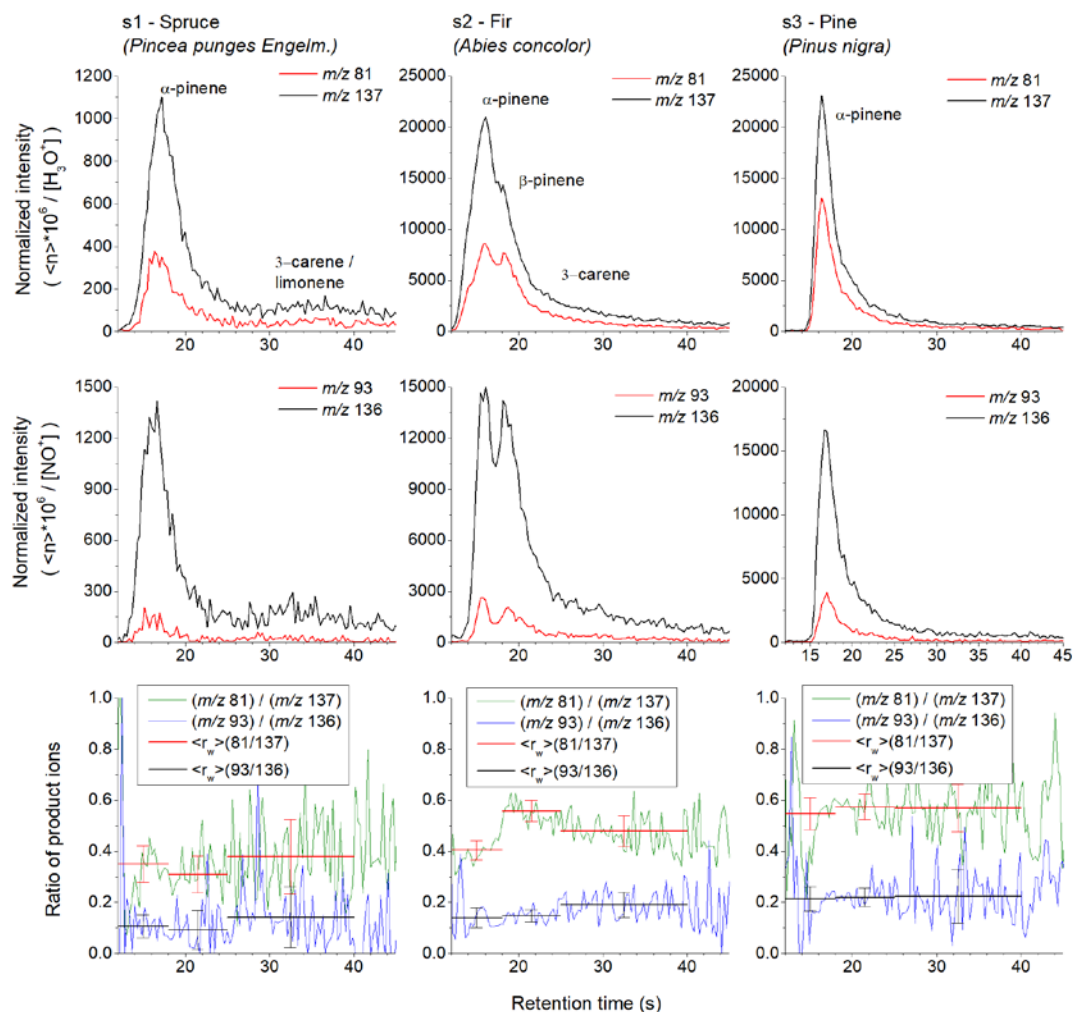
Figure 5: Chromatograms derived using the product ions for the reactions of H₃O⁺ (upper row) and NO⁺ (lower row) reagent ions with monoterpenes obtained for the three investigated pine tree samples (s1, s2 and s3) using the MXT-1 column. The signal intensities are the analyte ion count rates normalized to a reagent ion count rate of 10⁶ s⁻¹. The black and red curves represent C₆H₉⁺ (m/z 81) and C₁₀H₁₇⁺ (m/z 137) product ions for H₃O⁺ and C₇H₉⁺ (m/z 93) and C₁₀H₁₆⁺ (m/z 136) product ions for NO⁺ reagent ions. The last row shows calculated ratios of product ions rᵢ for both reagent ions (green and blue curves) and for peaks areas calculated $\overline{r_w}$ (red and black).
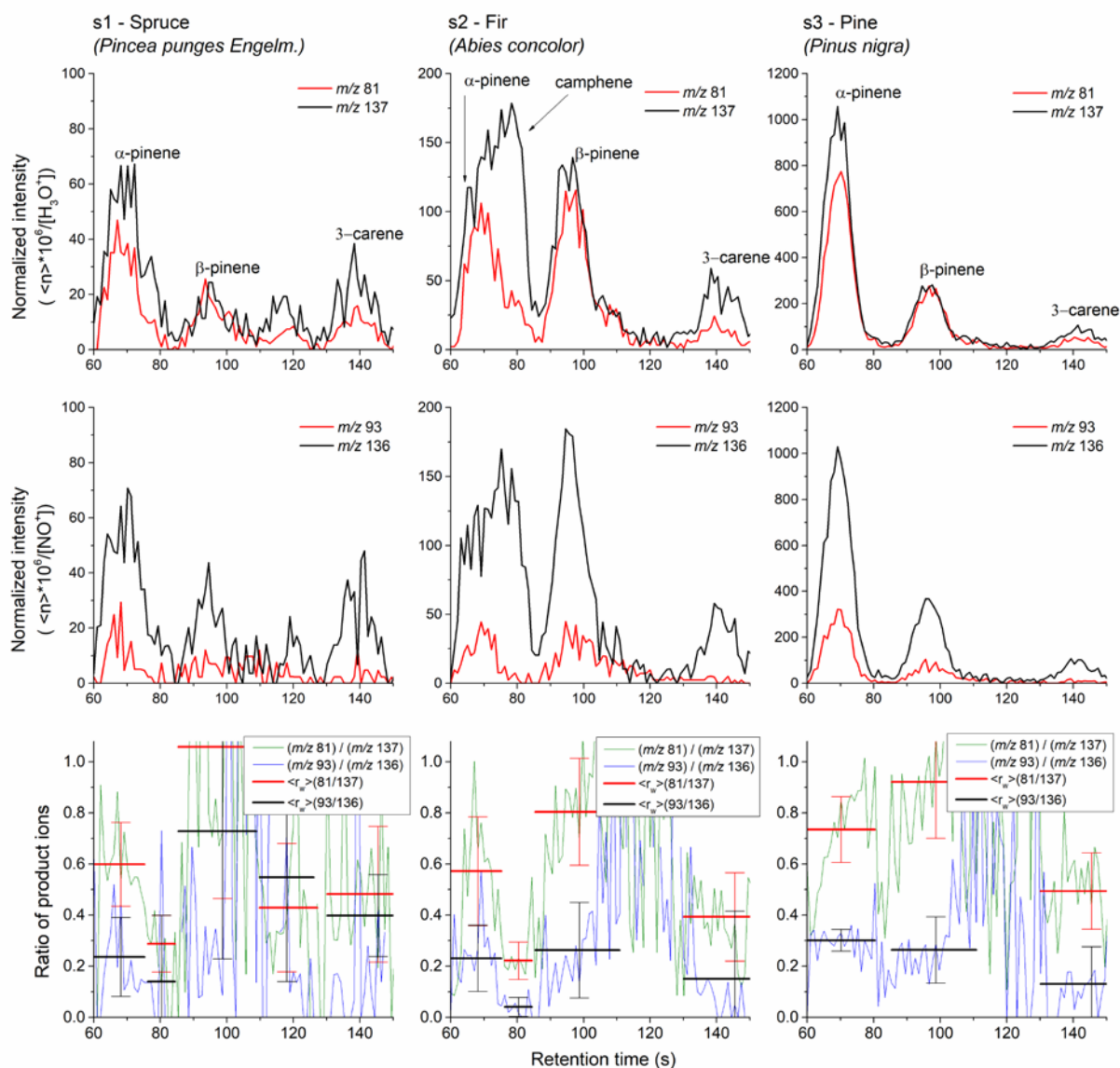
Figure 6: SIFT-MS selected ion mode/fast GC/SIFT-MS chromatograms for monoterpene emissions from pine tree samples (s1, s2 and s3) obtained using the MXT-Volatiles column. The upper and lower rows were obtained using H_3O^+ and NO^+ reagent ions respectively. The signal intensities are the analyte ion count rates normalized to a reagent ion count rate of 10^6 s^{-1}. The black and red curves stand for monitored ions $C_6H_9^+$ (m/z 81) and $C_{10}H_{17}^+$ (m/z 137) for H_3O^+ reagent ions of $C_7H_9^+$ (m/z 93) and $C_{10}H_{16}^+$ (m/z 136) for NO^+ reagent ions respectively. The last row shows calculated ratios of product ions r_i for both reagent ions (green and blue curves) and for peaks areas calculated $\overline{r_w}$ (red and black).

The chromatogram for the fir sample shows three peaks, where the first is due to both α-pinene and camphene. Transition of $\overline{r_w}$ from the left (0.57 for H_3O^+, 0.23 for NO^+) to the right (0.22 for H_3O^+, 0.04 for NO^+) part of the first peak is clearly visible in **Fig. 6** in middle column. The first peak of the fir sample thus consists of two isomers. The second peak is due to β-pinene ($\overline{r_w}$ 0.80 for H_3O^+, 0.26 for NO^+) and the third peak by 3-carene ($\overline{r_w}$ 0.39 for H_3O^+, 0.15 for NO^+).

5 The pine sample chromatogram shows three clear peaks of α-pinene (0.73 for H_3O^+, 0.30 for NO^+), β-pinene (0.92 for H_3O^+, 0.26 for NO^+) and 3-carene (0.49 for H_3O^+, 0.13 for NO^+) with just a very small and statistically insignificant indication of camphene. The retention times for α-pinene, β-pinene and 3-carene were 69.6 s, 97 s and 141 s, respectively.

Some differences can be seen between the results from the MXT-1 and MXT-Volatiles columns. The most significant difference is the presence of a camphene peak in the fir sample headspace, and the presence of β-pinene and 3-carene in the

10 pine sample headspace when the MXT-Volatiles column was used. However, samples were collected at different times of the year and the character of the samples was also different (only needles for MXT-1 and whole twigs for the MXT-Volatiles analyses).

4.5 Comparison with previous studies

The present experiments indicate that using the fast GC-SIFT-MS combination, it is possible to achieve only qualitative

15 analysis of the monoterpene mixture with a limit of the detection of about 100 ppb. This is inferior to the previously described fastGC-PTR-MS systems (Materić et al., 2015; Pallozzi et al., 2016), which achieved full separation with limit of the detection up to 1-2 ppt. However, one advantage of SIFT-MS is the facility to use two reagent ions, and the analysis of product ion ratios provides additional information. Thus, the combination of the data from the two reagent ions together with the analyses of the product ion signal ratios r_i can be shown to improve the identification of monoterpenes.

20 The results obtained from the present study agree well with the literature reports. In a previous study (Mumm et al., 2004) of the volatiles emitted by *Pinus nigra* needles, 35 terpenoid compounds were identified, with the following being most abundant: α-pinene (45%), β-phellandrene (9%), (R)-(+)-limonene (8%), β-pinene (5%) and 3-carene (2%). Holzke et al. (2006) studied diurnal and seasonal variation of monoterpenes and sesquiterpenes from Scots pine. The main isomers they observed were α-pinene, β-pinene and 3-carene, which represented 90% of the total terpene emission. A similar study on monoterpene emissions

25 from boreal Scots pine showed that the most abundant monoterpenes measured above the forest and from the canopy were α-pinene and 3-carene (Räisänen et al., 2009).

(Kainulainen et al., 1992) investigated the effect of drought and waterlogging stress on needle monoterpenes of *Picea abies* (spruce). In the controlled group, the most abundant monoterpenes were camphene (22%), (R)-(+)-limonene (14%), α-pinene (9%) and myrcene (6%). In the emission from Southern and Central Sweden (Janson, 1993) the following isomers were most

30 abundant: α -pinene (60-70%), camphene (10%), (R)-(+)-limonene (10%) and 3-carene (4%). (Zavarin et al., 1975) studied cortical oleoresin from *Abies concolor* (fir) that were collected in 43 different localities in order to analyse their composition for the monoterpenoid fractions. They concluded that the production of camphene and 3-carene varied geographically. In the study of (Pureswaran et al., 2004) they focused on quantitative variations in monoterpene vapours in four species of conifers,

concluding that the four species (Douglas-fir, Lodgepole pine, Interior spruce and Interior Fir) did not differ qualitatively but there were significant differences in their quantitative profiles. For example, Coastal Douglas fir needle samples contained 10% of α-pinene, 31% of Sabinene and 40% of β-pinene, and in samples of interior Douglas fir the most abundant isomers were bornyl acetate (26%), camphene (25%), α-pinene and β-pinene (both 15%). The present results thus agree with the usually

5   reported composition of terpenes emitted from pine trees and their parts.

5 Summary and conclusions

A new method has been developed that allows quantitative analyses of individual monoterpenes in mixtures using SIFT-MS enhanced by chromatographic pre-separation. As a pre-separation module, bespoke electrically heated fast GC systems were constructed by which pre-separation of the isomers was achieved in retention times shorter than 45 s for an MXT-1 column

10   and shorter than 180 s for an MXT-Volatiles column. Individual monoterpenes were identified and analysed by SIFT-MS from the ratios of the analyte ion signals generated in their reactions with H_3O^+ and NO^+ reagent ions. Thus, using both the SIFT-MS analyte ion ratios and the GC retention times, six monoterpenes in a mixture of eight were identified using the MXT-1 column whilst all eight monoterpenes were identified using the MXT-Volatiles column. To demonstrate the applicability of this unique analytical combination to real samples, the volatile monoterpenes in the headspace of spruce, fir and pine needles

15   were analysed. All headspace samples clearly contained α-pinene and a lower amount of β-pinene and 3-carene. A significant contribution of camphene was also observed in the fir needles sample headspace. A weakness of the current fast GC setup is the relatively poor temperature stability caused by a strong dependence on the laboratory ambient temperature. However, this can surely be improved by active temperature feedback to control the column temperature. It has been shown that a clear advantage of SIFT-MS is the facility to use different reagent ions and to utilize the ratios of the specific product ions of their

20   reactions with the various monoterpene isomers at the same retention time to improve the identification of the monoterpenes. In conclusion, the present study demonstrated that the combination of SIFT-MS determination of fragment ion fractions of the analyte reactions, together with low resolution GC pre-separation techniques, allows analyses of mixtures of monoterpenes in air in short time periods. This novel idea of a fast GC-SIFT-MS combination could broaden the application of SIFT-MS to *in situ* trace gas analyses of complex mixtures such as ambient air and exhaled breath.

25   **Data availability**

All data are available upon request from the corresponding author (Michal Lacko).

Author contribution

ML and NW crated experimental hardware and provided experiments with MXT-1 column, ML, KS and PP then provided experiments with MXT-Volatiles column. PS and ML provided data treatment and paper preparation.

Competing interests

5   The authors declare that they have no conflict of interest.

Acknowledgment

This project has received funding from the European Union's Horizon 2020 research and innovation programme under the Marie Skłodowska-Curie grant agreement No 674911. We also gratefully acknowledge partial funding from The Czech Science Foundation (GACR Project No. 17-13157Y). We would like to thank Professor David Smith for his advice and help

10   in the preparation of the manuscript.

References

Allardyce, R. A., Langford, V. S., Hill, A. L., and Murdoch, D. R.: Detection of volatile metabolites produced by bacterial growth in blood culture media by selected ion flow tube mass spectrometry (SIFT-MS), Journal of microbiological methods, 65, 361-365, 2006.

15   Amelynck, C., Schoon, N., and Dhooghe, F.: SIFT Ion Chemistry Studies Underpinning the Measurement of Volatile Organic Compound Emissions by Vegetation, Current Analytical Chemistry, 9, 540-549, 2013.

Atkinson, R., and Arey, J.: Gas-phase tropospheric chemistry of biogenic volatile organic compounds: a review, Atmospheric Environment, 37, 197-219, 2003.

Chameides, W., Fehsenfeld, F., Rodgers, M., Cardelino, C., Martinez, J., Parrish, D., Lonneman, W., Lawson, D., Rasmussen,

20   R., and Zimmerman, P.: Ozone precursor relationships in the ambient atmosphere, Journal of Geophysical Research: Atmospheres, 97, 6037-6055, 1992.

ChemicalBook: https://www.chemicalbook.com/ChemicalProductProperty_EN_CB4443087.htm, 2017, cited in January 2019.

OriginPro 9.0 OriginLab Corporation, One Roundhouse Plaza, Suite 303, Northampton, MA 01060, United States. 1800-969-

25   7720.: https://www.originlab.com/, 2018.

Daubert, T. E.: Physical and thermodynamic properties of pure chemicals: Data compilation Hemisphere Pub. Corp., New York, 1989.

de Gouw, J., and Warneke, C.: Measurements of volatile organic compounds in the earth's atmosphere using proton-transfer-reaction mass spectrometry, Mass Spectrometry Reviews, 26, 223-257, 2007.

Ellis, A. M., and Mayhew, C. A.: Proton transfer reaction mass spectrometry: principles and applications, John Wiley & Sons, 2013.

5 Fehsenfeld, F., Calvert, J., Fall, R., Goldan, P., Guenther, A. B., Hewitt, C. N., Lamb, B., Liu, S., Trainer, M., and Westberg, H.: Emissions of volatile organic compounds from vegetation and the implications for atmospheric chemistry, Global Biogeochemical Cycles, 6, 389-430, 1992.

Garcia, G. A., Nahon, L., and Powis, I.: Near-threshold photoionization spectroscopy of the mono-terpenes limonene and carvone, International Journal of Mass Spectrometry, 225, 261-270, 2003.

10 Haynes, W. M.: CRC handbook of chemistry and physics, CRC press, New York, 2014.

Holzke, C., Hoffmann, T., Jaeger, L., Koppmann, R., and Zimmer, W.: Diurnal and seasonal variation of monoterpene and sesquiterpene emissions from Scots pine (Pinus sylvestris L.), Atmospheric Environment, 40, 3174-3185, 2006.

Janson, R. W.: Monoterpene emissions from Scots pine and Norwegian spruce, Journal of geophysical research: atmospheres, 98, 2839-2850, 1993.

15 Jordan, A., Haidacher, S., Hanel, G., Hartungen, E., Herbig, J., Märk, L., Schottkowsky, R., Seehauser, H., Sulzer, P., and Märk, T. D.: An online ultra-high sensitivity Proton-transfer-reaction mass-spectrometer combined with switchable reagent ion capability (PTR+SRI−MS), International Journal of Mass Spectrometry, 286, 32-38, 2009.

Kainulainen, P., Oksanen, J., Palomäki, V., Holopainen, J., and Holopainen, T.: Effect of drought and waterlogging stress on needle monoterpenes of Picea abies, Canadian Journal of Botany, 70, 1613-1616, 1992.

20 Kulmala, M., Suni, T., Lehtinen, K., Maso, M. D., Boy, M., Reissell, A., Rannik, Ü., Aalto, P., Keronen, P., and Hakola, H.: A new feedback mechanism linking forests, aerosols, and climate, Atmospheric Chemistry and Physics, 4, 557-562, 2004.

Lindinger, W., Hansel, A., and Jordan, A.: On-line monitoring of volatile organic compounds at pptv levels by means of proton-transfer-reaction mass spectrometry (PTR-MS) medical applications, food control and environmental research, International Journal of Mass Spectrometry and Ion Processes, 173, 191-241, 1998.

25 Materić, D., Lanza, M., Sulzer, P., Herbig, J., Bruhn, D., Turner, C., Mason, N., and Gauci, V.: Monoterpene separation by coupling proton transfer reaction time-of-flight mass spectrometry with fast GC, Analytical and bioanalytical chemistry, 407, 7757-7763, 2015.

Matisová, E. and Dömötörová, M.: Fast gas chromatography and its use in trace analysis, Journal of Chromatography A, 1000, 199-221, 2003.

30 Mumm, R., Tiemann, T., Schulz, S., and Hilker, M.: Analysis of volatiles from black pine (Pinus nigra): significance of wounding and egg deposition by a herbivorous sawfly, Phytochemistry, 65, 3221-3230, 2004.

NIST WebBook Chemie, NIST Standard Reference Database Number 69, U.S. Secretary of Commerce, National Institute of Standards and Technology: Gaithersburg, MD: http://webbook.nist.gov/chemistry/ cited in January 2019.

Nolscher, A. C., Yanez-Serrano, A. M., Wolff, S., de Araujo, A. C., Lavric, J. V., Kesselmeier, J., and Williams, J.: Unexpected seasonality in quantity and composition of Amazon rainforest air reactivity, Nat Commun, 7, 10383, 2016.

Pallozzi, E., Guidolotti, G., Ciccioli, P., Brilli, F., Feil, S., and Calfapietra, C.: Does the novel fast-GC coupled with PTR-TOF-MS allow a significant advancement in detecting VOC emissions from plants? Agricultural and Forest Meteorology, 216, 232-240, 2016.

Pureswaran, D. S., Gries, R., and Borden, J. H.: Quantitative variation in monoterpenes in four species of conifers, Biochemical systematics and ecology, 32, 1109-1136, 2004.

Pysanenko, A., Španěl, P., and Smith, D.: Analysis of the isobaric compounds propanol, acetic acid and methyl formate in humid air and breath by selected ion flow tube mass spectrometry, SIFT-MS, International Journal of Mass Spectrometry, 285, 42-48, 2009.

Räisänen, T., Ryyppö, A., and Kellomäki, S.: Monoterpene emission of a boreal Scots pine (Pinus sylvestris L.) forest, Agricultural and forest meteorology, 149, 808-819, 2009.

Rinne, J., Ruuskanen, T. M., Reissell, A., Taipale, R., Hakola, H., and Kulmala, M.: On-line PTR-MS measurements of atmospheric concentrations of volatile organic compounds in a European boreal forest ecosystem, Boreal environment research, 10, 425-436, 2005.

Romano, A., Fischer, L., Herbig, J., Campbell-Sills, H., Coulon, J., Lucas, P., Cappellin, L., and Biasioli, F.: Wine analysis by Fast GC proton-transfer reaction-time-of-flight-mass spectrometry, International Journal of Mass Spectrometry, 369, 81-86, 2014.

Savitzky, A., and Golay, M. J.: Smoothing and differentiation of data by simplified least squares procedures, Anal. Chem., 36, 1627-1639, 1964.

Schoon, N., Amelynck, C., Vereecken, L., and Arijs, E.: A selected ion flow tube study of the reactions of H_3O^+, NO^+ and O_2^+ with a series of monoterpenes, International Journal of Mass Spectrometry, 229, 231-240, 2003.

Shestivska, V., Antonowicz, S. S., Dryahina, K., Kubišta, J., Smith, D., and Španěl, P.: Direct detection and quantification of malondialdehyde vapour in humid air using selected ion flow tube mass spectrometry supported by gas chromatography/mass spectrometry, Rapid Communications in Mass Spectrometry, 29, 1069-1079, 2015.

Shestivska, V., Nemec, A., Dřevínek, P., Sovová, K., Dryahina, K., and Španěl, P.: Quantification of methyl thiocyanate in the headspace of Pseudomonas aeruginosa cultures and in the breath of cystic fibrosis patients by selected ion flow tube mass spectrometry, Rapid Communications in Mass Spectrometry, 25, 2459-2467, 2011.

Shestivska, V., Spanel, P., Dryahina, K., Sovova, K., Smith, D., Musilek, M., and Nemec, A.: Variability in the concentrations of volatile metabolites emitted by genotypically different strains of Pseudomonas aeruginosa, Journal of Applied Microbiology, 113, 701-713, 2012.

Smith, D., Španěl, P., Holland, T. A., Al Singari, W., and Elder, J. B.: Selected ion flow tube mass spectrometry of urine headspace, Rapid communications in mass spectrometry, 13, 724-729, 1999.

Smith, D., and Španěl, P.: Selected ion flow tube mass spectrometry (SIFT-MS) for on-line trace gas analysis, Mass spectrometry reviews, 24, 661-700, 2005.

Smith, D., and Španěl, P.: Ambient analysis of trace compounds in gaseous media by SIFT-MS, Analyst, 136, 2009-2032, 2011a.

5 Smith, D., and Španěl, P.: Direct, rapid quantitative analyses of BVOCs using SIFT-MS and PTR-MS obviating sample collection, TrAC Trends in Analytical Chemistry, 30, 945-959, 2011b.

Smith, D., Sovová, K., and Španěl, P.: A selected ion flow tube study of the reactions of H_3O^+, NO^+ and $O_2^{+\bullet}$ with seven isomers of hexanol in support of SIFT-MS, International Journal of Mass Spectrometry, 319, 25-30, 2012.

Song, M., Xia, Y., and Tomasino, E.: Investigation of a Quantitative Method for the Analysis of Chiral Monoterpenes in White

10 Wine by HS-SPME-MDGC-MS of Different Wine Matrices, Molecules, 20, 7359-7378, 2015.

Španěl, P., Ji, Y., and Smith, D.: SIFT studies of the reactions of H_3O^+, NO^+ and O_2^+ with a series of aldehydes and ketones, International journal of mass spectrometry and ion processes, 165, 25-37, 1997.

Španěl, P., and Smith, D.: Selected ion flow tube studies of the reactions of H_3O^+, NO^+, and O_{2+} with several aromatic and aliphatic hydrocarbons, International Journal of Mass Spectrometry, 181, 1-10, 1998.

15 Španěl, P., Davies, S., and Smith, D.: Quantification of breath isoprene using the selected ion flow tube mass spectrometric analytical method, Rapid communications in mass spectrometry, 13, 1733-1738, 1999.

Španěl, P., Dryahina, K., and Smith, D.: A general method for the calculation of absolute trace gas concentrations in air and breath from selected ion flow tube mass spectrometry data, International Journal of Mass Spectrometry, 249-250, 230-239, 2006.

20 Španěl, P., and Smith, D.: Advances in On-line Absolute Trace Gas Analysis by SIFT-MS, Curr. Anal. Chem., 9, 525-539, 2013.

Takasago: http://www.takasago.com/cgi-bin/pdf/alphaterpinene.pdf, 2011, cited in January 2019.

Tani, A., Hayward, S., and Hewitt, C.: Measurement of monoterpenes and related compounds by proton transfer reaction-mass spectrometry (PTR-MS), International Journal of Mass Spectrometry, 223, 561-578, 2003.

25 TGSC, The Good Scents Company Information System: http://www.thegoodscentscompany.com/, cited in January 2019.

Thompson, J. M., and Perry, D. B.: A new system of refillable and uniquely identifiable diffusion tubes for dynamically generating VOC and SVOC standard atmospheres at ppm and ppb concentrations for calibration of field and laboratory measurements, Journal of Environmental Monitoring, 11, 1543-1544, 2009.

Van Kempen, G. M. P., and Van Vliet, L. J.: Mean and variance of ratio estimators used in fluorescence ratio imaging,

30 Cytometry Part A, 39, 300-305, 2000.

Wang, T., Španěl, P., and Smith, D.: Selected ion flow tube, SIFT, studies of the reactions of H_3O^+, NO^+ and $O2^+$ with eleven $C_{10}H_{16}$ monoterpenes, Int. J. Mass Spec., 228, 117-126, 2003.

Yaws, C. L.: Handbook of Vapor Pressure. Vol 3: C8-C28 Compounds, Gulf Pub Co., Houston, 1994.

Zavarin, E., Snajberk, K., and Fisher, J.: Geographic variability of monoterpenes from cortex of Abies concolor, Biochemical Systematics and Ecology, 3, 191-203, 1975.